Supplementary Tables

Supplementary Table S1 Origin, RRID and seeding densities for cell viability assay of used cell lines. Cell lines were obtained from German Collection of Microorganisms and Cell Cultures (DSMZ) or American Type Culture Collection (ATCC).

Cell Line	Source	Cat #	Date of Acquisition	RRID	Density
Jurkat	DSMZ	ACC 282	2019/06/13	RRID:CVCL_0065	10k
SUP-T11	DSMZ	ACC 605	2018	RRID:CVCL_2210	15k
Loucy	ATCC	CRL-2629	2019	RRID:CVCL_1380	10k
DERL-2	DSMZ	ACC 531	2017/01/18	RRID:CVCL_2016	75k
HH	DSMZ	ACC 707	2020	RRID:CVCL_1280	5k
SR786			2019/01/30	RRID:CVCL_1711	20k
Daudi	DSMZ	ACC 78	2020/09/09	RRID:CVCL_0008	7k
Oci-Ly1	DSMZ	ACC 722	2020/09/09	RRID:CVCL_1879	20k

Supplementary Table S2 Primer sequences for EZH2 knockdown.

shRNA	Sigma-Aldrich TRC-Clone ID	Target Sequence
HH EZH2 KD1	TRCN0000040077	CCCAACATAGATGGACCAAAT
HH EZH2 KD2	TRCN0000353069	TATGATGGTTAACGGTGATCA
HH mock shRNA	SHC002	CAACAAGATGAAGAGCACCAA
Jurkat EZH2 KD1	TRCN0000040075	CCAACACAAGTCATCCCATTA
Jurkat EZH2 KD2	TRCN0000353069	TATGATGGTTAACGGTGATCA
Jurkat mock shRNA	SHC002	CAACAAGATGAAGAGCACCAA

Supplementary Table S3 RT-qPCR primer sequences.

Target	5'-forward Primer-3'	5'-reverse Primer-3'
ABCG1	CGCTTTCTCGGTCGGCA	CTGGGCTTCCGTGAGGTTAT
ABCG2	TCAGGAGGCCTTGGGATACT	AGGCTCTATGATCTCTGTGGC
EZH1	AACCCAACACTTCCCCTTGC	ACTGAACAGGTTGGACACGA
EZH2	GCAATTATTCTTTTCATGCAACACC	TTGGTGGGGTCTTTATCCGC
SREBF1	AGGGCGGGCGCAGAT	GGTTGTTGATAAGCTGAAGCATGT
SREBF2	GGCTGAAGAATAGGAGTTGCC	AACGGTCATTCACCCAGGTC
TBP	AGGAGCCAAGAGTGAAGAACAG	AGGAGAACAATTCTGGGTTTGA

Supplementary Table S4 Mutation and expression status of used cell lines. Data was acquired from Cosmic [accessed 2022/06/03] for Jurkat, Loucy, HH, SR786, and Daudi, from DepMap [accessed 2022/09/20] for SUPT11 and DERL-2, and from Morin *et al.* and Wright *et al.* for Oci-Ly1 [35, 50-53].

Background		**Jurkat**	**SUPT11**	**Loucy**
T-cell origin, immature		Cortical T-ALL	ETP-ALL	ETP-ALL
PRC2 Complex	EZH2	wt, high expression	wt, wt expression	wt, silenced
	EZH1	p.R557H, low expression	wt, wt expression	wt, wt expression
	H3K27me3	wt trimethylation	wt trimethylation	no trimethylation
	EED	wt	wt	wt
	SUZ12	p.R516H p.Q737Tfs*20	wt	wt
	RbAp48	p.A294T	wt	wt
DNA Damage Response	Tp53	p.R196*	p.R213*	p.V272M
	p21	wt	wt	wt
	ATM	wt	wt	wt
	ATR	p.R1631H p.I1264M	wt	wt
	MDM2	wt	wt	wt
Ras/Raf	SRC	wt	wt	wt
	Nras	wt	wt	wt
	Nras1	wt	wt	wt
	Raf1	p.A237T	wt	wt
	Araf	wt	p.A475P	wt
	Braf	p.A728V	wt	wt
Apoptosis Suppression	Casp2	wt	wt	wt
	Casp3	p.E190D	wt	wt
	Casp6	wt	wt	wt
	Casp7	wt	wt	wt
	Casp8	p.L107R	wt	wt
	Casp9	wt	wt	wt
	Casp10	p.V33Sfs*12	wt	wt
	LMNA	p.R166W p.Q293* p.R388H p.R482Q	wt	wt
	LMNB1	wt	wt	wt
	LMNB2	wt	wt	wt
	ICAD	wt	wt	wt
	PARP1	wt	wt	wt
	Pak2	p.S508N	wt	p.S508N
ABC Transporters	ABCG1	p.D587N p.D587N	wt	wt
	ABCG2	wt	wt	wt
	ABCB1	wt	wt	wt
	ABCC1	wt	wt	wt
	ABCC2	p.H823Y	wt	wt
	ABCC3	p.Q614Rfs*34	wt	wt
	ABCC4	wt	wt	wt
	ABCC5	wt	wt	wt
	ABCC6	wt	wt	wt
	ABCC10	wt	wt	wt
SREBF	SREBF1	wt	wt	wt
	SREBF2	p.R896C p.E328Kfs*26	wt	wt

Background		**DERL-2**	**HH**	**SR786**
T-cell origin, mature		HSTCL	CTCL	ALK+ ALCL
PRC2 Complex	EZH2	wt, high expression	wt, wt expression	wt, wt expression
	EZH1	wt, high expression	wt, high expression	wt, high expression
	H3K27me3	no trimethylation	wt trimethylation	wt trimethylation
	EED	wt	wt	wt
	SUZ12	wt	wt	wt
	RbAp48	wt	wt	wt
DNA Damage Response	Tp53	wt	c.560-1G>A	p.P152L
	p21	wt	wt	wt
	ATM	wt	wt	wt
	ATR	wt	wt	wt
	MDM2	wt	wt	wt
Ras/Raf	SRC	wt	wt	wt
	Nras	wt	wt	wt
	Nras1	wt	wt	wt
	Raf1	wt	wt	wt
	Araf	wt	wt	wt
	Braf	wt	wt	wt
Apoptosis Suppression	Casp2	wt	wt	wt
	Casp3	wt	wt	wt
	Casp6	wt	wt	wt
	Casp7	wt	wt	wt
	Casp8	wt	wt	wt
	Casp9	wt	wt	wt
	Casp10	wt	wt	wt
	LMNA	wt	wt	wt
	LMNB1	wt	wt	wt
	LMNB2	wt	wt	wt
	ICAD	wt	wt	wt
	PARP1	wt	wt	wt
	Pak2	wt	wt	wt
ABC Transporters	ABCG1	wt	wt	wt
	ABCG2	wt	wt	wt
	ABCB1	wt	wt	wt
	ABCC1	wt	wt	wt
	ABCC2	wt	wt	wt
	ABCC3	wt	wt	wt
	ABCC4	wt	wt	wt
	ABCC5	wt	wt	wt
	ABCC6	wt	wt	wt
	ABCC10	wt	wt	wt
SREBF	SREBF1	wt	wt	wt
	SREBF2	wt	p.P870R p.D582N	wt

Background		**Oci-Ly1**	**Daudi**
B-cell origin, mature		GC-DLBCL	Burkitt Lymphoma
PRC2 Complex	EZH2	p.Y641N, high expression	wt, wt expression
	EZH1	wt, wt expression	wt, high expression
	H3K27me3	high trimethylation	wt trimethylation
	EED	wt	wt
	SUZ12	wt	wt
	RbAp48	wt	wt
DNA Damage Response	Tp53	p.R158H	p.G266E
	p21	wt	wt
	ATM	wt	wt

	ATR	wt	p.F2427L
	MDM2	wt	wt
Ras/Raf	SRC	wt	wt
	Nras	wt	wt
	Nras1	wt	wt
	Raf1	wt	wt
	Araf	wt	wt
	Braf	wt	wt
Apoptosis Suppression	Casp2	wt	wt
	Casp3	wt	wt
	Casp6	wt	wt
	Casp7	wt	wt
	Casp8	wt	wt
	Casp9	wt	wt
	Casp10	wt	wt
	LMNA	wt	wt
	LMNB1	wt	wt
	LMNB2	wt	wt
	ICAD	wt	wt
	PARP1	wt	wt
	Pak2	wt	wt
ABC Transporters	ABCG1	wt	wt
	ABCG2	wt	wt
	ABCB1	wt	wt
	ABCC1	wt	wt
	ABCC2	wt	wt
	ABCC3	wt	wt
	ABCC4	E936Q	wt
	ABCC5	wt	p.S523T p.V476F
	ABCC6	wt	wt
	ABCC10	wt	wt
SREBF	SREBF1	wt	wt
	SREBF2	wt	wt

Abbreviations: T-ALL – T-cell acute lymphoblastic leukemia: ETP-ALL – early T-cell precursor acute lymphoblastic leukemia; HSTCL – hepatosplenic T-cell lymphoma; CTCL – cutaneous T-cell lymphoma; ALK+ ALCL – anaplastic large cell lymphoma, ALK-positive; GC-DLBCL – diffuse large B-cell lymphoma, germinal center-like.

Supplementary Figures

Supplementary Figure S1

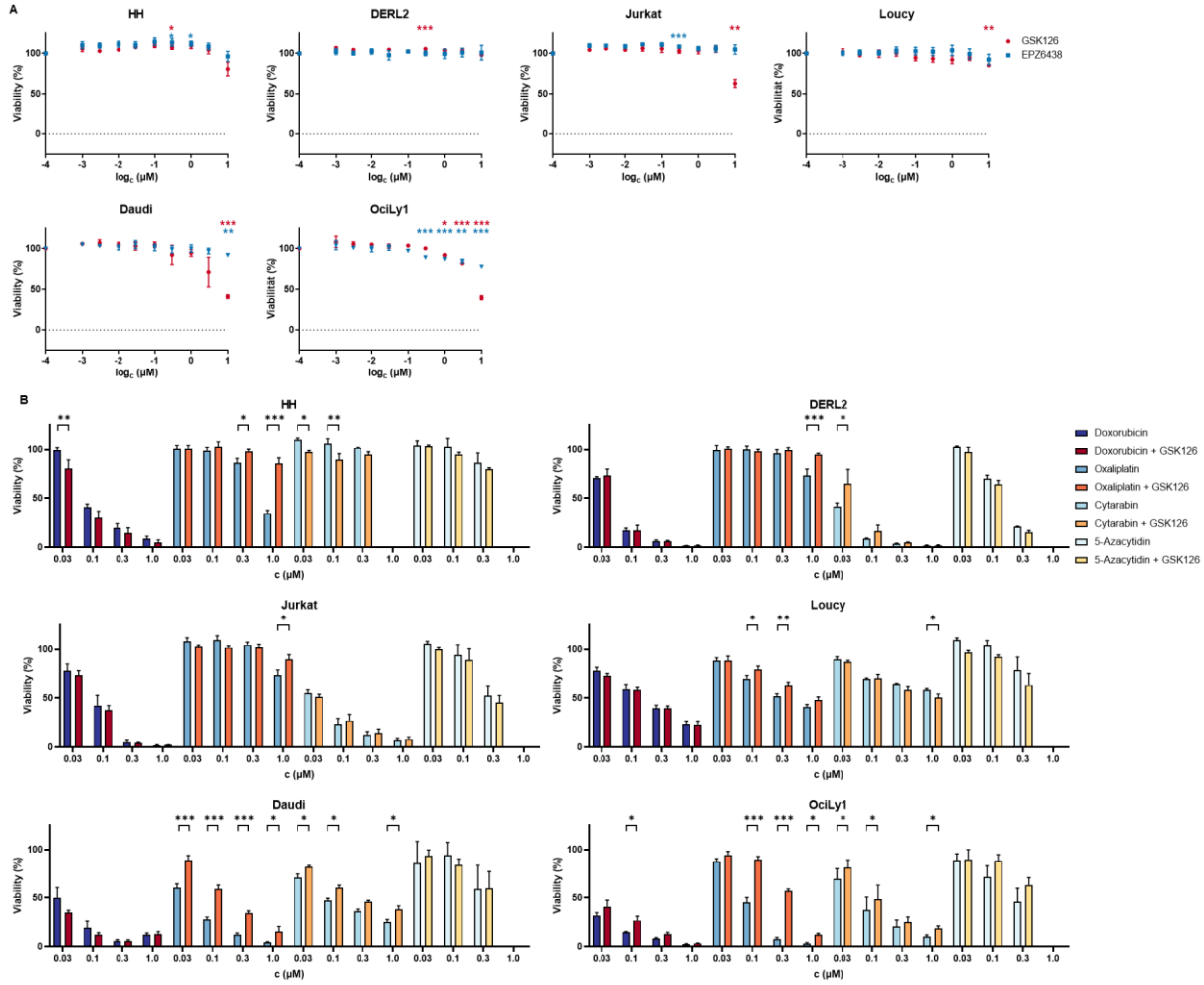

Supplementary Figure S1 SAM-competitive EZH2 inhibitors are not sufficient as single agent but modify chemotherapy sensitivity. A Both GSK126 and EPZ6438 were evaluated for reduction of cell viability at clinically relevant concentrations after 72 h of incubation in cell viability assays. Significant differences between the untreated control and under GSK126 (red) or EPZ6438 (blue) incubation are indicated by the respective coloured asterisks. Each point represents mean ± SEM, n=3. **B** In a screening approach, sensitivity towards the respective chemotherapeutic as single agent or in combination with GSK126 was evaluated. Each bar represents the mean ± SEM, n=3 (* p≤0.05; ** p≤0.005; *** p≤0.001).

Supplementary Figure S2

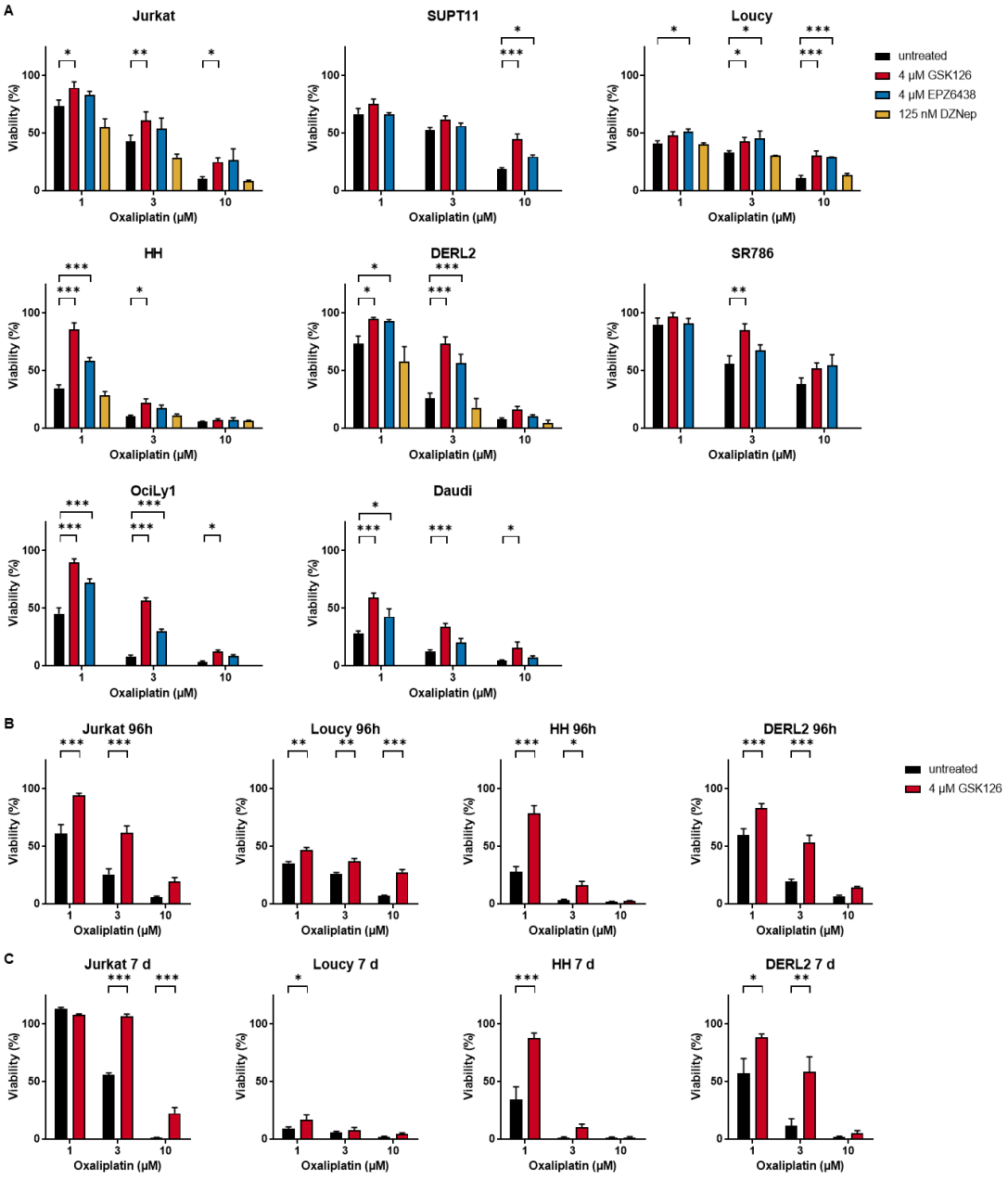

Supplementary Figure S2 SAM-competitive EZH2 inhibitors increase oxaliplatin resistance significantly. A Both GSK126 and EPZ6438 were able to induce oxaliplatin resistance in a broad panel of cell lines after 72 h of incubation in oxaliplatin cell viability assays. Oxaliplatin resistance persisted in a representative subset of cell lines after (**B**) 96 h and (**C**) 7 d of combinational incubation with GSK126. Each bar represents the mean ± SEM, n=3 (* p≤0.05; ** p≤0.005; *** p≤0.001).

Supplementary Figure S3

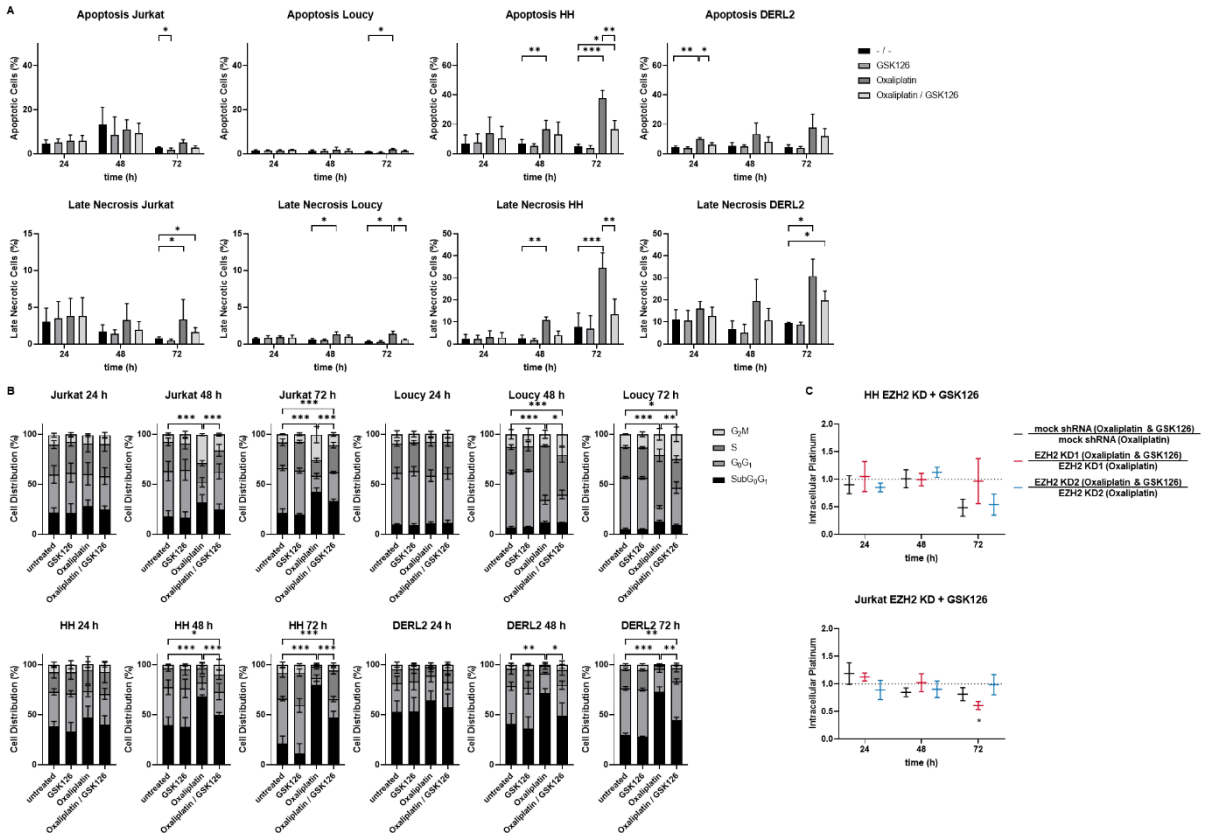

Supplementary Figure S3 Mechanistic changes under pharmacological EZH2 inhibition or EZH2 knockdown. Pharmacological EZH2 Inhibition reduces the oxaliplatin induced (**A**) apoptosis and necrosis as well as (**B**) cell cycle deregulation. Each bar represents the mean ± SD, n=3. **C** In ICP-MS, the intracellular platinum content was reduced by pharmacological EZH2 inhibition even under EZH2 knockdown. The values were normed to the respective shRNA cell line oxaliplatin monotherapy. Each line represents the mean ± SEM, n=3 (* $p \leq 0.05$; ** $p \leq 0.005$; *** $p \leq 0.001$).

Supplementary Figure S4

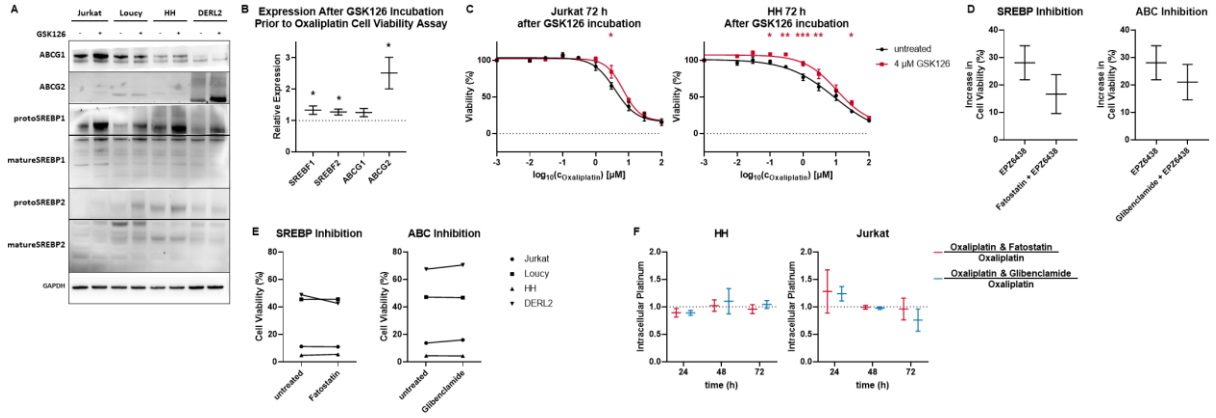

Supplementary Figure S4 RNA sequencing validation on protein level, sequential pharmacological EZH2 inhibition and SREBP and ABC inhibition validation. A Proteins found to be differentially expressed by pharmacological EZH2 inhibition were validated by westernblot. **B** Pharmacological EZH2 inhibition by GSK126 was confirmed by upregulation of SRE binding proteins and ABC transporters after 72 h of treatment. Each line represents the mean of the exemplary cell lines Jurkat and HH ± SEM, n=3 per cell line. C Oxaliplatin cell viability assay after pharmacological EZH2 inhibition by GSK126 treatment again was able to induce oxaliplatin resistance after 72 h of sequential incubation. Each point represents the mean ± SEM, n=3. **D** In oxaliplatin viability assay, reduction of oxaliplatin resistance by inhibition of SRE binding proteins or ABC transporters was confirmed by pharmacological EZH2 inhibition by EPZ6438 in combined analysis. For comparison the oxaliplatin concentration of the maximal induced resistance by pharmacological EZH2 inhibition of each respective cell line was chosen. Each line represents the mean of the exemplary cell lines Jurkat, Loucy and HH ± SEM, n=3 per cell line. **E** In oxaliplatin cell viability assays, neither Fatostatin nor Glibenclamide were able to alter oxaliplatin sensitivity. For comparison the oxaliplatin concentration of the maximal induced resistance by pharmacological EZH2 inhibition of each respective cell line was chosen. Each point represents the mean of n=3. **F** The intracellular platinum content, measured by ICP-MS, was not altered by Fatostatin or Glibenclamide. For comparison, values of combination approaches were normed to the respective oxaliplatin monotherapy control. Each line represents the mean ± SEM, n=3.

Supplementary Figure S5

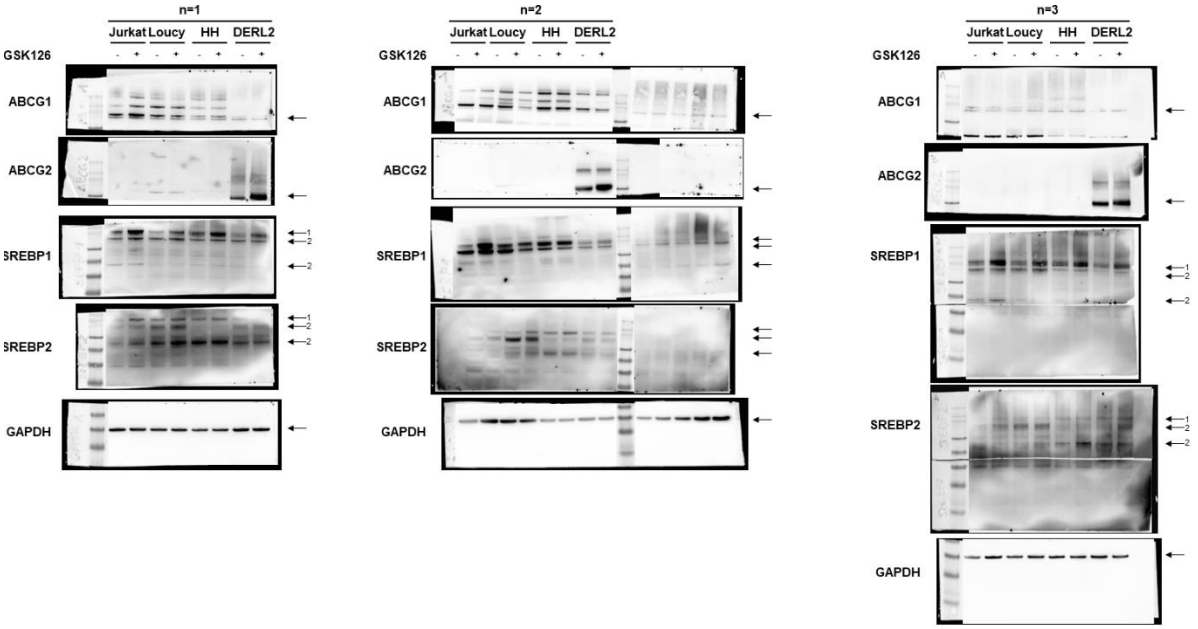

Supplementary Figure S5 Original westernblot data of RNA sequencing data validation. Arrows indicate the correct protein band. Probes that were not related to the validation are not labelled. Arrow specifications: 1 – protoSREBP1/2. 2 – matureSREBP1/2.

Supplementary Figure S6

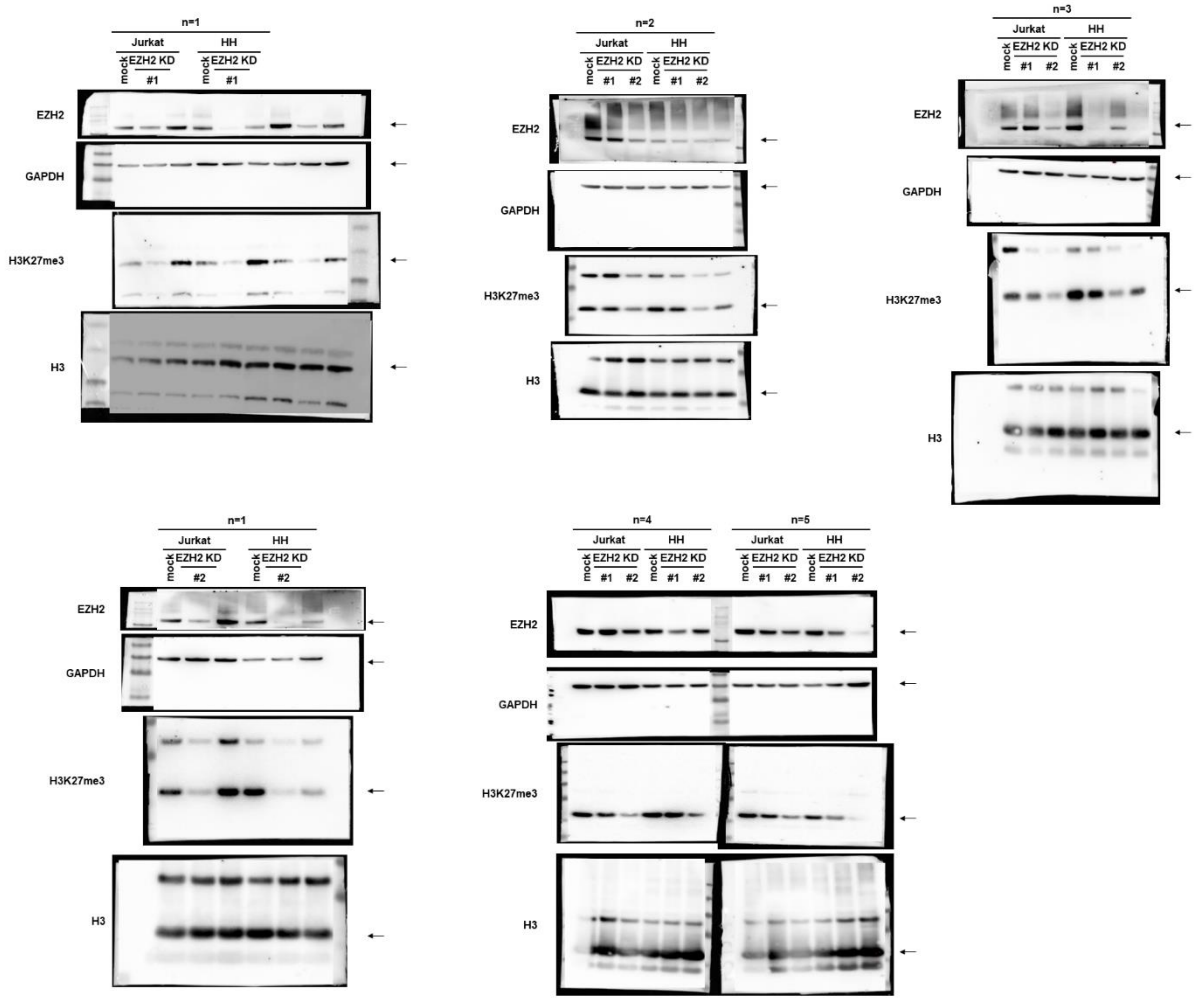

Supplementary Figure S6 Original westernblot data of RNA sequencing data validation. Arrows indicate the correct protein band. Probes of EZH2 knockdown cell lines that were not further used are not labelled.

Supplementary Figure S7

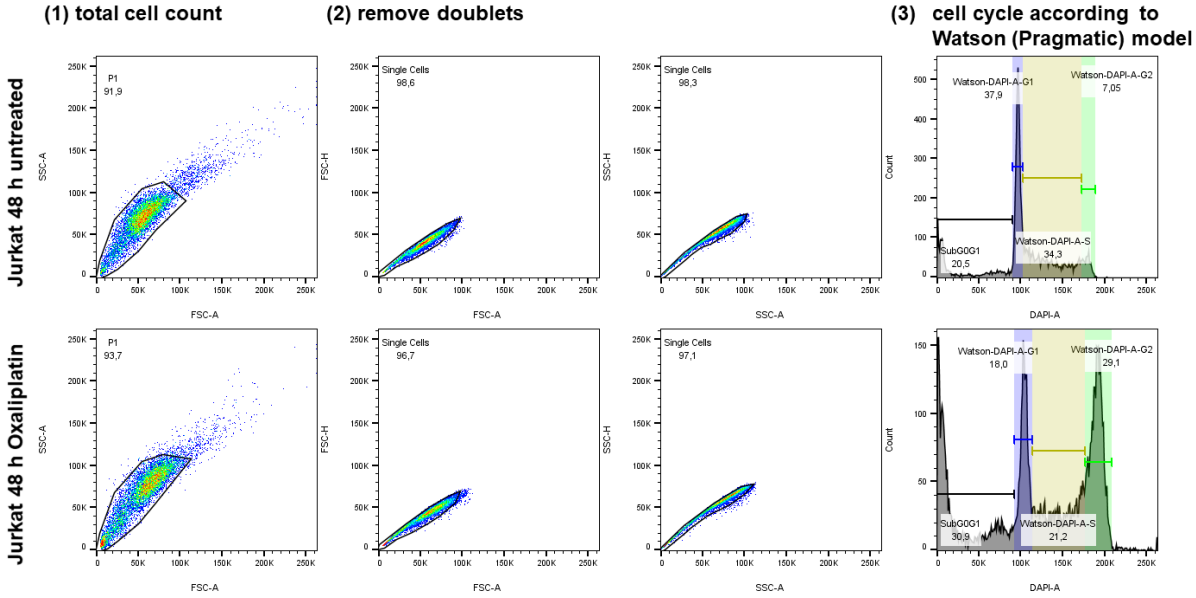

Supplementary Figure S7 Exemplary gating strategy for cell cycle analysis. The data is shown for the samples Jurkat untreated and Jurkat oxaliplatin treated, each after 48 h of incubation.

Supplementary Figure S8

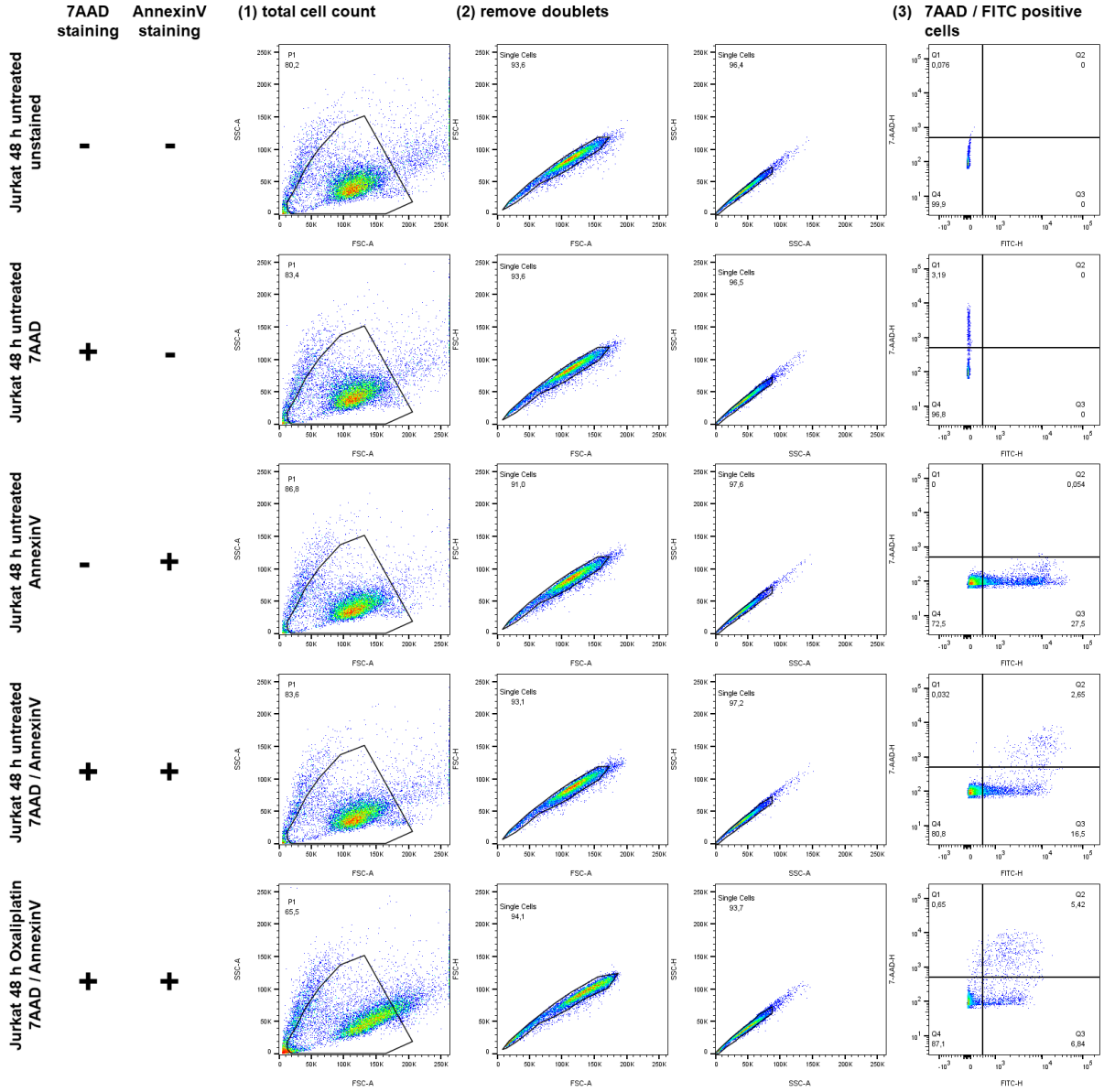

Supplementary Figure S8 Exemplary gating strategy for cell cycle analysis. The data is shown for the samples Jurkat untreated and Jurkat oxaliplatin treated, each after 48 h of incubation. 7AAD- and AnnexinV-positivity was examined per cell line by evaluating unstained control, 7AAD-stained control, and AnnexinV-stained control. The according gates were used for each sample of the respective cell line of the experiment.

Supplementary References

35. Morin, R.D.; Johnson, N.A.; Severson, T.M.; Mungall, A.J.; An, J.; Goya, R.; Paul, J.E.; Boyle, M.; Woolcock, B.W.; Kuchenbauer, F.; et al. Somatic mutations altering EZH2 (Tyr641) in follicular and diffuse large B-cell lymphomas of germinal-center origin. Nat. Genet. 2010, 42, 181–185.

50. Tate, J.G.; Bamford, S.; Jubb, H.C.; Sondka, Z.; Beare, D.M.; Bindal, N.; Boutselakis, H.; Cole, C.G.; Creatore, C.; Dawson, E.; et al. COSMIC: The Catalogue of Somatic Mutations in Cancer. Nucleic Acids Res. 2019, 47, D941–D947.

51. Barretina, J.; Caponigro, G.; Stransky, N.; Venkatesan, K.; Margolin, A.A.; Kim, S.; Wilson, C.J.; Lehár, J.; Kryukov, G.V.; Sonkin, D.; et al. The Cancer Cell Line Encyclopedia enables predictive modelling of anticancer drug sensitivity. Nature 2012, 483, 603–607.

52. Morin, R.; Mungall, K.; Pleasance, E.; Mungall, A.; Goya, R.; Huff, R.; Scott, D.W.; Ding, J.; Roth, A.; Chiu, R.; et al. Mutational and structural analysis of diffuse large B-cell lymphoma using whole-genome sequencing. Blood 2013, 122, 1256–1265.

53. Wright, G.W.; Huang, D.W.; Phelan, J.D.; Coulibaly, Z.A.; Roulland, S.; Young, R.M.; Wang, J.Q.; Schmitz, R.; Morin, R.D.; Tang, J.; et al. A Probabilistic Classification Tool for Genetic Subtypes of Diffuse Large B Cell Lymphoma with Therapeutic Implications. Cancer Cell 2020, 37, 551–568.e14.